Pergamon

PII: S1359-6454(96)00392-8

Acta mater. Vol. 45, No. 7, pp. 2911–2920, 1997

Published by Elsevier Science Ltd

1359-6454/97 $17.00 + 0.00

KINETICS OF THE SIMULTANEOUS DECOMPOSITION OF AUSTENITE INTO SEVERAL TRANSFORMATION PRODUCTS

S. J. JONES and H. K. D. H. BHADESHIA

University of Cambridge, Department of Materials Science and Metallurgy, Pembroke Street, Cambridge CB2 3QZ, U.K.

(Received 25 September 1996)

Abstract—Transformations in steels rarely occur in isolation. This paper describes a modification of the Avrami overall transformation kinetics theory as adapted by Cahn, for grain boundary nucleated phases. The modification deals with the simultaneous occurrence of two or more transformations. The method is demonstrated to faithfully reproduce published data on the volume fractions of allotriomorphic, Widmanstätten ferrite and pearlite as a function of chemical composition, austenite grain size and heat treatment (isothermal or continuous cooling transformation). © *1997 Acta Metallurgica Inc.*

INTRODUCTION

Almost all commercial steels are produced using heat-treatments in which the austenite cools continuously through the transformation temperature range. This usually leads to a final microstructure which is a mixture of many transformation products, because the high-temperature austenite can decompose into a large variety of ferritic transformation products, each of which can form by a different mechanism. These reactions may overlap and interact with each other, either by "hard"-impingement in which adjacent particles touch, or by "soft"-impingement where their diffusion or thermal fields overlap [1]. The interactions are known to be important in determining the final microstructure.

It follows that in order to model the development of microstructure, it is necessary to develop a theory capable of handling simultaneous, interacting precipitation reactions. The evolution of volume fraction during solid-state transformation is usually described using the classical Johnson–Mehl–Avrami theory, which has been reviewed thoroughly by Christian [1]. The present work deals with a general extension of this theory to multiple reactions, which is then applied to explain published data on steels. In particular, structural steels frequently have a microstructure consisting of allotriomorphic ferrite, Widmanstätten ferrite and pearlite. Although a great deal is known about allotriomorphic ferrite and pearlite, kinetic theory for Widmanstätten ferrite is rather limited. An understanding of Widmanstätten ferrite is important because it is a phase which greatly influences the mechanical properties of steels. There are many investigations which suggest that Widmanstätten ferrite can be detrimental to toughness [2]. It tends to grow in packets of parallel plates across which cracks tend to propagate without much deviation.

Watson and McDougall [3] demonstrated that the growth of Widmanstätten ferrite leads to a change in the shape of the transformed region. This shape deformation is an invariant-plane strain (IPS) with a large shear component, which is characteristic of displacive transformation. Carbon nevertheless has to partition into the austenite during the growth of Widmanstätten ferrite. The transformation is therefore a paraequilibrium displacive transformation with the growth rate controlled by the diffusion of carbon in the austenite ahead of the plate tip, with an appropriate allowance made for the strain energy due to the IPS shape change [4]. The nucleation mechanism of Widmanstätten ferrite is understood to the extent that it is possible to calculate the transformation start temperature (W_S) and the rate as a function of undercooling below W_S [5, 6]. It should therefore be possible to estimate the overall transformation kinetics as a function of the steel composition and heat treatment.

It is emphasised that Widmanstätten ferrite rarely occurs in isolation. It is usually preceded by the formation of allotriomorphic ferrite at the austenite grain surfaces and there may be other transformations such as pearlite which compete for untransformed austenite [7]. To deal with this complexity, we begin with a brief introduction to the classical Johnson–Mehl–Avrami model, in order to set the scene for the modifications made to allow for simultaneous reactions.

OVERALL TRANSFORMATION KINETICS

A given precipitate particle of the phase β effectively forms after an incubation period τ. Assuming growth at a constant rate G, the volume w_τ of a spherical particle is given by

$$w_\tau = (4\pi/3)G^3(t-\tau)^3 \quad (t > \tau) \qquad (1)$$

with $w_\tau = 0$ for $(t < \tau)$ where t is the time defined from the instant the sample reaches the isothermal transformation temperature.

Particles nucleated at different locations may eventually touch; this problem of hard impingement is neglected at first, by allowing particles to grow through each other and by permitting nucleation to happen even in regions which have already transformed. The calculated volume of the β phase is therefore an *extended volume*. The change in extended volume due to particles nucleated in a time interval $t = \tau$ to $t = \tau + \mathrm{d}\tau$ is, therefore,

$$\mathrm{d}V_\beta^e = w_\tau I V \, \mathrm{d}\tau$$

$$V_\beta^e = (4\pi V/3)\int_{\tau=0}^{t} G^3 I (t-\tau)^3 \, \mathrm{d}\tau \qquad (2)$$

where I is the nucleation rate per unit volume and V is the total sample volume.

Only those parts of the change in extended volume which lie in untransformed regions of the parent phase can contribute to the change in real volume of β. If nucleation occurs randomly in the parent material then the probability that any change in extended volume lies in the untransformed parent phase is proportional to the fraction of untransformed material at that instant. It follows that the actual change in volume in the time interval t to $t + \mathrm{d}t$ is

$$\mathrm{d}V_\beta = \left(1 - \frac{V_\beta}{V}\right)\mathrm{d}V_\beta^e$$

so that

$$V_\beta^e = -V \ln\left(1 - \frac{V_\beta}{V}\right)$$

and

$$-\ln\left(1 - \frac{V_\beta}{V}\right) = (4\pi/3)G^3 \int_0^t I(t-\tau)^3 \, \mathrm{d}\tau. \qquad (3)$$

For a constant nucleation rate, integration of equation (3) gives the familiar Johnson–Mehl–Avrami equation:

$$\zeta_\beta = \frac{V_\beta}{V} = 1 - \exp\left(-\frac{1}{3}\pi G^3 I t^4\right) \qquad (4)$$

where ζ_β is the volume fraction of β.

This approach is limited to the precipitation of a single phase; it can be applied to cases where more than one decomposition reaction occurs, if the individual reactions occur over different temperature ranges, i.e. they occur successively and largely independently [8, 9]. This is not the case in practice. The adaptation of the Johnson–Mehl–Avrami approach to deal with many reactions occurring simultaneously is illustrated with a simple example below.

SIMPLE SIMULTANEOUS REACTIONS: RANDOM DISTRIBUTION OF NUCLEATION SITES

The principles involved are first illustrated with a simplified example in which α and β precipitate at the same time from the parent phase which is designated γ. It is assumed that the nucleation and growth rates do not change with time and that the particles grow isotropically.

The increase in the extended volume due to particles nucleated in a time interval $t = \tau$ to $t = \tau + \mathrm{d}\tau$ is, therefore, given by

$$\mathrm{d}V_\alpha^e = \tfrac{4}{3}\pi G_\alpha^3 (t-\tau)^3 I_\alpha V \, \mathrm{d}\tau$$

and

$$\mathrm{d}V_\beta^e = \tfrac{4}{3}\pi G_\beta^3 (t-\tau)^3 I_\beta V \, \mathrm{d}\tau \qquad (5)$$

where G_α, G_β, I_α and I_β are the growth and nucleation rates of α and β, respectively, all of which are assumed here to be independent of time. V is the total volume of the system. For each phase, the increase in extended volume will consist of three separate parts. Thus, for α the parts are:

(a) α which forms in untransformed γ;
(b) α which forms in existing α;
(c) α which forms in existing β.

Only α formed in untransformed γ will contribute to the real volume of α. On average, a fraction $[1 - (V_\alpha + V_\beta)/V]$ of the extended volume will be in the previously untransformed material. It follows that the increase in real volume of α in the time interval t to $t + \mathrm{d}t$ is given by

$$\mathrm{d}V_\alpha = \left(1 - \frac{V_\alpha + V_\beta}{V}\right)\mathrm{d}V_\alpha^e$$

and similarly for β,

$$\mathrm{d}V_\beta = \left(1 - \frac{V_\alpha + V_\beta}{V}\right)\mathrm{d}V_\beta^e.$$

In general, V_α will be some complex function of V_β and it is not possible to *analytically* integrate these expressions to find the relationship between the real and extended volumes, although they can, of course, be integrated *numerically*. However, in certain simple cases it is possible to relate V_α to V_β by multiplication with a suitable constant, K, in which case $V_\beta = KV_\alpha$ and analytical integration becomes possible.

The equations relating the increment in the real volume to that of the extended volume can therefore be written as

$$dV_\alpha = \left(1 - \frac{V_\alpha + KV_\alpha}{V}\right) dV_\alpha^e$$

and

$$dV_\beta = \left(1 - \frac{V_\beta + KV_\beta}{KV}\right) dV_\beta^e. \quad (6)$$

They may then be integrated to find an analytical solution relating the extended and real volumes analogous to that for single-phase precipitation:

$$\frac{V_\alpha^e}{V} = \frac{-1}{1+K} \ln\left[1 - \frac{V_\alpha}{V}(1+K)\right]$$

and

$$\frac{V_\beta^e}{V} = \frac{-K}{1+K} \ln\left[1 - \frac{V_\beta}{V}\left(\frac{1+K}{K}\right)\right]. \quad (7)$$

The total extended volume fraction is found for each phase by integrating equation (5) with respect to τ. This gives:

$$\zeta_\alpha = \left(\frac{1}{1+K}\right)\left(1 - \exp\left[-\frac{1}{3}(1+K)\pi G_\alpha^3 I_\alpha t^4\right]\right) \quad (8)$$

$$\zeta_\beta = \left(\frac{K}{1+K}\right)\left(1 - \exp\left[-\frac{1}{3}\left(\frac{1+K}{K}\right)\pi G_\beta^3 I_\beta t^4\right]\right). \quad (9)$$

These equations resemble the well-known Avrami equation for single-phase precipitation with extra factors to account for the presence of a second precipitate phase. When the volume fraction of both precipitating phases is very small the equations approximate to the expressions for each phase precipitating alone. This is because nearly all of the extended volume then lies in previously untransformed material and contributes to the real volume. As simultaneous precipitation proceeds, the predicted volume fraction of each phase becomes less than that predicted if the phases were precipitating alone. This is expected, because additional phases reduce the fraction of the extended volume which lies in previously untransformed material.

Since the nucleation and growth rates were assumed to be constant, it is possible to calculate explicitly the value of K, which is given by

$$K = V_\beta / V_\alpha = (I_\beta G_\beta^3)/(I_\alpha G_\alpha^3).$$

An example calculation for the case of linear (i.e. constant) growth is presented in Fig. 1, for the case where the growth rate of β is set to be twice that of α (with identical nucleation rates). The final volume fraction of the β phase is eight times that of the α phase because volume fraction is a function of the growth rate cubed.

Whereas the analytical method is more satisfying, numerical methods are more amenable to changes in the boundary conditions during transformation, as described below.

COMPLEX SIMULTANEOUS REACTIONS

The analytical expressions discussed above for simultaneous reactions rely on the assumptions of constant nucleation and growth rates, which are not appropriate for the present purposes. The nucleation and growth rate of allotriomorphic ferrite, Widmanstätten ferrite and pearlite may change with the progress of the transformation as the composition of the austenite and/or the temperature changes whilst the nucleation sites are grain surfaces.

There are two applications of the Avrami extended space idea for grain boundary nucleated reactions, the first applying to the gradual elimination of free grain boundary area and the second to the gradual elimination of volume of untransformed material [10]. If we consider a boundary of area O_B (which is equal to the total grain boundary area of the sample) in a system with n precipitating phases, where $O_{i,y}$ is the total real area intersected by the ith phase on a plane parallel to the boundary but at a distance y normal to that boundary at the time t, we have for the jth phase,

$$\Delta O_{j,y} = \left(1 - \frac{\sum_{i=1}^{n} O_{i,y}}{O_B}\right) \Delta O_{j,y}^e \quad (10)$$

where $\Delta O_{j,y}$ is the change in the real area intersected with the plane at y by the phase j, during the small time interval t to $t + \Delta t$. $\Delta O_{j,y}^e$ is similarly, the change in *extended* area of intersection with the same plane at y. This may have a contribution from particles nucleated throughout the period $t = 0$ to $t = m\,\Delta t$, where m is an integer such that $m\,\Delta t$ is the current

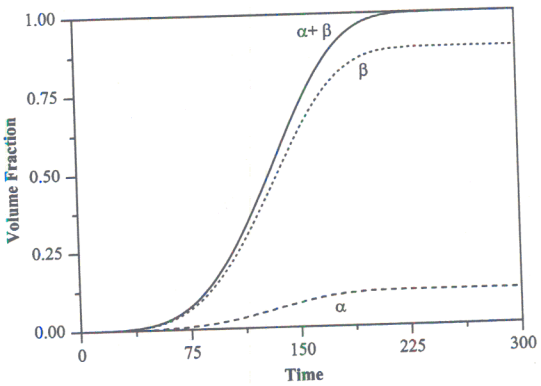

Fig. 1. Simultaneous precipitation of β and α. Identical nucleation rates but with β particles growing at twice the rate of the α particles.

time, so that

$$\Delta O^{e}_{j,y} = O_B \sum_{k=0}^{m} (I_{j,k}\, \Delta\tau A_{j,k,y}\, \Delta t)$$

where $A_{j,k,y}$ is the rate of change of area of intersection on plane y of a particle of the phase j which nucleated at $\tau = k\,\Delta\tau$ at the current time $t = m\,\Delta t$. $I_{j,k}$ is the nucleation rate per unit area of the phase j during the time interval $t = k\,\Delta\tau$ to $t = k\,\Delta\tau + \Delta\tau$. Note that Δt and $\Delta\tau$ are taken to be numerically identical and the number of extended particles nucleated in this time interval is therefore $O_B I_{j,k}\,\Delta\tau$. $\Delta O_{j,y}$ is then used to update the total real area of intersection of the phase j with the same plane at y at the time $t + \Delta t$ by writing

$$O_{j,y,t+\Delta t} = O_{j,y,t} + \Delta O_{j,y} \quad \text{for} \quad j = 1 \ldots n.$$

To obtain a change in the extended volume of the phase j on one side of the boundary, it is necessary to integrate as follows:

$$\mathrm{d}V^{e}_{j} = \int_{y=0}^{q_j^{\max}} \mathrm{d}O_{j,y}\, \mathrm{d}y$$

where the integrand $\mathrm{d}O_{j,y}$ is equivalent to $\Delta O_{j,y}$ and $q_j^{\max}$ is the maximum *extended size* of a particle of phase j in a direction normal to the grain boundary plane. Thus the change in the extended volume of the phase j on one side of the boundary in the time interval t to $t + \Delta t$ may be numerically evaluated as

$$\Delta V^{e}_{j} = \Delta y \sum_{y=0}^{q_j^{\max}} \Delta O_{j,y} \qquad (11)$$

where Δy is a small interval in y. Therefore, the corresponding change in real volume after allowing for impingement with particles originating from other boundaries is

$$\Delta V_j = \left(1 - \frac{\sum_{i=1}^{n} V_i}{V}\right) \Delta V^{e}_{j} \qquad (12)$$

where V_i is the real volume of the ith phase at the time t. The instantaneous value of ΔV_j, together with corresponding changes in the volumes of the other $n-1$ phases, can be used to calculate the total volume of each phase at the time $t + \Delta t$ in a computer implemented numerical procedure by writing

$$V_{j,t+\Delta t} = V_{j,t} + \Delta V_j \quad \text{for} \quad j = 1 \ldots n$$

so that a plot of the fraction of each phase can be obtained as a function of time. The growth and nucleation rates can also be updated during this step, should they have changed because of solute enrichment in the untransformed parent material or because there is a change in temperature during continuous cooling transformation.

The next section explains how these equations apply to allotriomorphic ferrite, Widmanstätten ferrite and pearlite. These phases are henceforth identified by setting the phase index as $j = 1$, 2 or 3, respectively; these subscripts are also used in identifying the nucleation and growth rates of the phases concerned.

ALLOTRIOMORPHIC FERRITE

Classical nucleation theory is used to model the nucleation of allotriomorphic ferrite, with the grain boundary nucleation rate per unit area given by:

$$I_1 = C_a \frac{kT}{h} \exp\left\{-\frac{G^* + Q}{RT}\right\} \exp\left\{-\frac{\tau^*}{t}\right\} \qquad (13)$$

where h is the Planck constant, k is the Boltzmann constant, $C_a = 1.214 \times 10^{12}\ \mathrm{m}^{-2}$ is a fitted constant [11], R is the universal gas constant and $Q = 200$ kJ/mol is a constant activation energy representing the barrier to the transfer of atoms across the interface. The activation energy for nucleation, $G^* = C_b\sigma^3/\Delta G^2$, where $\sigma = 0.022\ \mathrm{J/m^2}$ represents the interfacial energy per unit area, $C_b = 5.58$ is another fitted constant and ΔG is the maximum chemical free energy change per unit volume available for nucleation [12]. The second exponential term relates to the achievement of a steady-state nucleation rate; $\tau^* = n_c^2 h(4a_c kT)^{-1} \exp\{Q/RT\}$, where n_c is the number of atoms in the critical nucleus and a_c is the number of atoms in the critical nucleus which are at the interface [1].

The nucleation and growth of allotriomorphic ferrite has been described by modelling the allotriomorphs as discs having their faces parallel to the nucleating grain boundary plane [13]. The discs are assumed to grow on both sides of the parent boundary under paraequilibrium conditions, so that the half-thickness q_1 of each disc during isothermal growth is given by:

$$q_1 = \zeta(t - \tau)^{1/2} \qquad (14)$$

where ζ is the one-dimensional parabolic thickening rate constant. The growth rate slows down as the concentration gradient ahead of the moving interface decreases to accommodate the carbon that is partitioned into the austenite. The growth rate parallel to the grain boundary plane is taken to be three times that normal to it, giving a constant aspect ratio η_1 of 3.0, so that the disc radius is $\eta_1 q_1$ [14].

For non-isothermal growth the change in thickness during a time interval $\mathrm{d}t$ is given by differentiating equation (14):

$$\mathrm{d}q_1 = \tfrac{1}{2}\zeta(t - \tau)^{-1/2}\, \mathrm{d}t.$$

Therefore, for a particle nucleated at $\tau = k\,\Delta\tau$ the half thickness at the time $(m+1)\,\Delta t$ is evaluated numerically as:

$$q_{1,(m+1)\Delta t} = q_{1,m\Delta t} + \tfrac{1}{2}\zeta(m\,\Delta t - k\,\Delta\tau)^{-1/2}\,\Delta t.$$

The rate of change of area of intersection on a plane y of a disc of phase 1 (allotriomorphic ferrite) nucleated at $\tau = k\,\Delta\tau$ at the time $m\,\Delta t$ is:

$$A_{1,k,y} = \pi\eta_1^2\zeta^2 \qquad (q_{1,(m+1)\Delta t} > y)$$

$$A_{1,k,y} = \pi\eta_1^2 q_{1,(m+1)\Delta t}^2/\Delta t \qquad (q_{1,(m+1)\Delta t} = y)$$

$$A_{1,k,y} = 0 \qquad (q_{1,(m+1)\Delta t} < y).$$

Since the ferrite allotriomorphs can grow into both of the adjacent austenite grains, it follows from equation (11) that

$$\Delta V_1^e = 2\,\Delta y \sum_{y=0}^{q_1^{\max}} \Delta O_{1,y}. \qquad (15)$$

The parabolic rate constant is obtained by solving the equation [1]:

$$2\left(\frac{\underline{D}}{\pi}\right)^{1/2}\Omega = \zeta\,\exp\left\{\frac{\zeta^2}{4\underline{D}}\right\}\mathrm{erfc}\left\{\frac{\zeta}{2\underline{D}^{1/2}}\right\}$$

with

$$\Omega = \frac{x^{\gamma\alpha} - \bar{x}}{x^{\gamma\alpha} - x^{\alpha\gamma}}$$

and where $x^{\gamma\alpha}$ and $x^{\alpha\gamma}$ are the paraequilibrium carbon concentrations in austenite and ferrite, respectively, at the interface (obtained using a calculated multicomponent phase diagram), $\bar{x}$ is the average carbon concentration in the alloy and $\underline{D}$ is a weighted average diffusivity [15] of carbon in austenite, given by:

$$\underline{D} = \int_{x^{\gamma\alpha}}^{\bar{x}} \frac{D\{x\}\,\mathrm{d}x}{\bar{x} - x^{\gamma\alpha}}$$

where D is the diffusivity of carbon in austenite at a particular concentration of carbon.

WIDMANSTÄTTEN FERRITE

There is fine detail in *TTT* (time–temperature–transformation) diagrams, but they consist essentially of two C-curves (Fig. 2). One of these represents reconstructive transformations at elevated temperatures where atoms are mobile within the time scale of the usual experiments on steels. The lower temperature C-curve represents displacive transformations such as Widmanstätten ferrite and bainite.

The lower C-curve has a flat top; the temperature corresponding to this flat top is identified as T_h, the highest temperature at which displacive transformation occurs during isothermal heat-treatment. T_h is either the Widmanstätten ferrite start (W_S) or bainite-start (B_S) temperature depending on the driving force available at T_h for the steel concerned.

Figure 3 shows two plots; the first is a calculation of the driving force for the paraequilibrium nucleation of ferrite at T_h, allowing carbon to partition between the austenite and ferrite. The second is the case where there is no partitioning at all during the nucleation of ferrite.

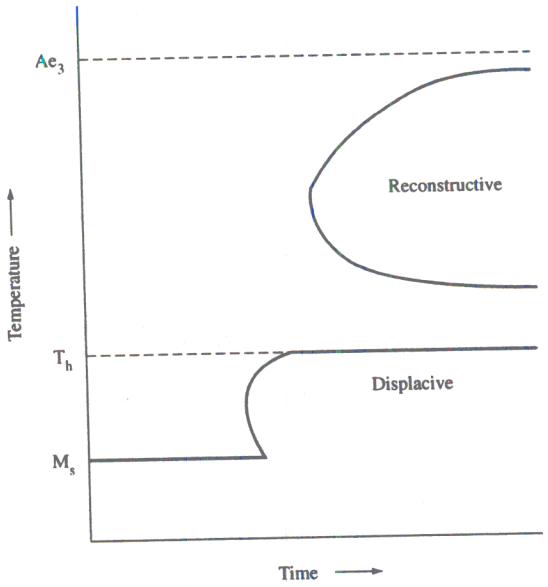

Fig. 2. Schematic *TTT* diagram illustrating the two C-curves and the T_h temperature.

It is evident that the nucleation of Widmanstätten ferrite or bainite cannot in general occur without the partitioning of carbon. The second interesting point is that the curve illustrated in Fig. 3(a) is linear. This straight line, which represents all steels, is henceforth called the *universal* G_N *function* and is

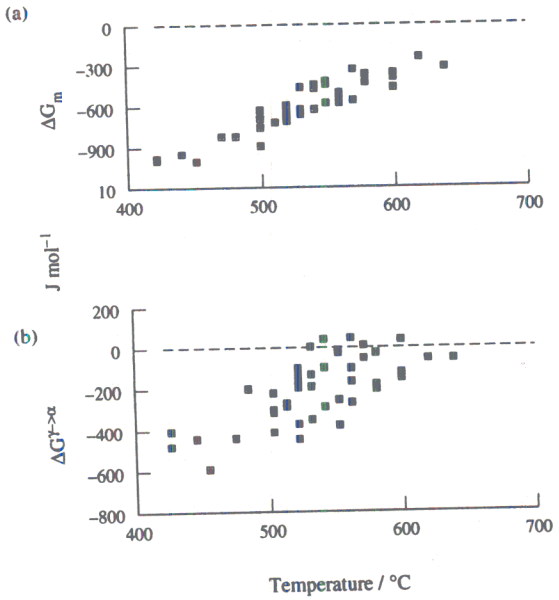

Fig. 3. Curves representing the free energy change necessary in order to obtain a detectable degree of transformation to Widmanstätten ferrite or bainite [5]. Note that each point represents a different steel. (a) The free energy change assuming paraequilibrium nucleation. (b) The free energy change assuming partitionless nucleation.

Table 1. Chemical composition (wt%)

C	Si	Mn	Cu	V
0.18	0.18	1.15	0.09	<0.003
P	S	Nb	Al	N
0.015	0.030	<0.005	0.026	0.0073

given by:

$$G_N = 3.637(T - 273.18) - 2540 \quad \text{(J/mol)} \quad (16)$$

with G_N giving the minimum free energy change necessary to nucleate Widmanstätten ferrite or bainite in any steel [5].

As explained elsewhere [5], a linear relation such as this cannot be explained by nucleation based on heterophase fluctuations. Consider a nucleation rate (I) equation:

$$I \propto \nu \exp(-G^*/kT) \quad (17)$$

where ν is an attempt frequency and all the other terms have their usual meanings. When this is rearranged, we get

$$-G^* \propto \beta T \quad (18)$$

where $\beta = k \ln\{I/\nu\}$. Consequently, the G_N vs T relation can only be linear if

$$G^* \propto G_N \quad (19)$$

and not the inverse square relationship implied by classical nucleation theory. This is entirely consistent with the theory for martensitic nucleation [5, 16].

What then are the conditions which determine whether at T_h, it is Widmanstätten ferrite that forms first or bainite? In order for a phase to form, it must nucleate and grow. Nucleation will occur at T_h when the driving force for nucleation becomes less than G_N:

$$\Delta G \leqslant G_N. \quad (20)$$

The nucleated phase can develop into Widmanstätten ferrite if a further condition is satisfied, that the driving force for paraequilibrium growth exceeds the stored energy of Widmanstätten ferrite, which amounts to about 50 J/mol [4, 5].

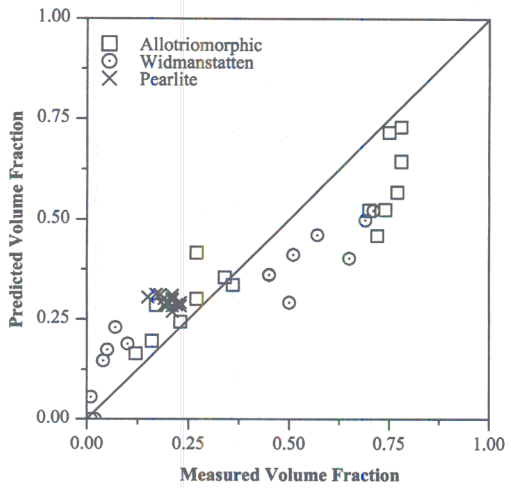

Fig. 4. A comparison of the calculated volume fraction vs experimental data reported by Bodnar and Hansen.

For the theory presented here, the nucleation rate per unit area for phase 2 (Widmanstätten ferrite) is given by

$$I_2 = \frac{1}{2C_c} \exp\left\{-\frac{C_d}{RT} - \frac{C_d \Delta G}{C_e RT}\right\} \quad (21)$$

where $C_c = 6.78 \times 10^{-10}$ m^2 s, $C_d = 2.065 \times 10^4$ J/mol and $C_e = 2540$ J/mol, all of which are constants determined by fitting to experimental data [17]. The equation applies below the Widmanstätten ferrite start temperature.

Trivedi has given a solution for the problem of the diffusion-controlled growth of plates [18]. The shape of the plates is taken to be that of a parabolic cylinder and is assumed to be constant throughout growth. The plate lengthening rate (V_2) at a temperature T for steady-state growth is obtained by solving the equation:

$$\Omega = (\pi p)^{0.5} \exp\{p\}\text{erfc}\{p^{0.5}\}[1 + (r_c/r)\Omega S_2\{p\}] \quad (22)$$

where the Péclet number p, which is a dimensionless velocity, is given by $p = V_2 r/2\underline{D}$. The weighted-average diffusion coefficient for carbon in austenite is used as before, but with the integral evaluated over the range $\bar{x}$ to x_r, where x_r is the carbon concentration in the austenite at the plate tip. x_r may significantly differ from the equilibrium carbon concentration $x^{\gamma\alpha}$ because of the Gibbs–Thompson capillarity effect [1] which allows for the change in equilibrium concentration as a function of interface curvature; x_r decreases as interface curvature increases, and growth ceases at a critical plate tip radius r_c when $x_r = \bar{x}$. For a finite plate tip radius (r),

$$x_r = x^{\gamma\alpha}[1 + (\Gamma/r)] \quad (23)$$

where Γ is the capillarity constant [1] given by

$$\Gamma = \frac{\sigma V_m}{RT} \frac{(1 - x^{\gamma\alpha})/(x^{\alpha\gamma} - x^{\gamma\alpha})}{1 + [\text{d}(\ln \Gamma_C)/\text{d}(\ln x^{\gamma\alpha})]} \quad (24)$$

where σ is the interface energy per unit area, taken to be 0.2 J/m^2, Γ_C is activity coefficient of carbon in austenite, and V_m = molar volume of ferrite. Note that for Widmanstätten ferrite, the paraequilibrium concentrations (e.g. $x^{\gamma\alpha}$) are calculated after allowing for the 50 J/mol of stored energy [5].

This assumes that the α composition is unaffected by capillarity, since $x^{\alpha\gamma}$ is always very small. r_c can be obtained by setting $x_r = \bar{x}$. The function $S_2\{p\}$ depends on the Péclet number; it corrects for variations in composition due to changing curvature along the interface and has been numerically evaluated by Trivedi [18]. Consistent with experimental data, we have also assumed the Zener hypothesis that the plate tip adopts a radius which is consistent with the maximum rate of growth [5].

The plates of Widmanstätten ferrite were modelled as tetragonal prisms, the longest dimension of which

Table 2. Details of the data plotted in Fig. 4. α and α_w represent the allotriomorphic ferrite and Widmanstätten ferrite fractions, respectively. The measured fractions are due to Bodnar and Hansen

γ grain size (μm)	Cooling rate (K/min)	α measured	α calculated	α_w measured	α_w calculated	Pearlite measured	Pearlite calculated
30	101	0.46	0.72	0.23	0.07	0.31	0.21
30	59	0.525	0.74	0.174	0.05	0.301	0.21
30	30	0.645	0.78	0.056	0.01	0.298	0.21
30	16	0.717	0.75	0	0.02	0.283	0.23
30	11	0.73	0.78	0	0.01	0.269	0.21
55	99	0.285	0.17	0.403	0.65	0.311	0.18
55	59	0.336	0.36	0.362	0.45	0.301	0.19
55	30	0.417	0.27	0.292	0.5	0.291	0.23
55	16	0.523	0.7	0.189	0.1	0.287	0.2
55	11	0.568	0.77	0.147	0.04	0.285	0.19
100	101	0.165	0.12	0.523	0.71	0.312	0.17
100	59	0.196	0.16	0.499	0.69	0.305	0.15
100	30	0.244	0.23	0.462	0.57	0.293	0.2
100	16	0.301	0.27	0.412	0.51	0.286	0.22
100	11	0.355	0.34	0.361	0.45	0.283	0.21

is given by $q_2 = V_2(t - \tau)$ during unhindered isothermal growth. For non-isothermal transformation,

$$q_{2,(m+1)\Delta t} = q_{2,m\Delta t} + V_2\,\Delta t.$$

The rate of change of area of intersection on a plane at a distance y from the austenite grain boundary is therefore:

$$A_{2,k,y} = 2\eta_2 V_2^2(m\,\Delta t - k\,\Delta\tau) \quad (q_{2,(m+1)\Delta t} > y)$$

$$A_{2,k,y} = \eta_2 q_{2,(m+1)\Delta t}^2/\Delta t \quad (q_{2,(m+1)\Delta t} = y)$$

$$A_{2,k,y} = 0 \quad (q_{2,(m+1)\Delta t} < y)$$

where η_2 is the ratio of the length to the thickness of the Widmanstätten ferrite plate, taken to be 0.02. Since the plates grow by displacive transformation, they can only grow into one of the adjacent austenite grains, so that the change in the extended volume (ΔV_2^e) is given directly by equation (11).

PEARLITE

The nucleation of pearlite is treated as for allotriomorphic ferrite but with a nucleation rate which is two orders of magnitude smaller. This is achieved by reducing the number density of nucleation sites.

The growth of pearlite was approximated to occur by a paraequilibrium mechanism, although it never in practice grows in this way. It is also assumed that the majority of diffusion occurs in the austenite just ahead of the transformation front. In these circumstances, the growth rate is given by [19]

$$V_3 = \frac{D}{g}\frac{s^2}{s_\alpha s_\theta}\frac{x^{\gamma\alpha} - x^{\gamma\theta}}{x^{\theta\gamma} - x^{\alpha\gamma}}\frac{1}{s}\left[1 - \frac{s_C}{s}\right] \qquad (25)$$

where θ represents cementite, α the ferrite within the pearlite and γ the austenite. g is a geometric factor equal to 0.72 in plain carbon steels, s is the interlamellar spacing, whose critical value at which growth stops is s_C and s_α, s_θ are the respective thickness of ferrite and cementite lamellae. The values of s and s_C are estimated empirically [20] and it is assumed that s adopts a value consistent with the maximum rate of growth.

Like allotriomorphic ferrite, pearlite growth occurs by a reconstructive mechanism and is not restricted by the presence of a grain boundary. The shape of pearlite colony is taken to be that of a disc (aspect ratio $\eta_3 = 1$) of half-thickness

$$q_3 = V_3(t - \tau) \quad \text{with} \quad q_{3,(m+1)\Delta t} = q_{3,m\Delta t} + V_3\,\Delta t.$$

The rate of change of area of intersection on a test-plane located at a distance y is given by

$$A_{3,k,y} = 2\pi\eta_3^2 V_3^2(m\,\Delta t - k\,\Delta\tau) \quad (q_{3,(m+1)\Delta t} > y)$$

$$A_{3,k,y} = \pi\eta_3^2 q_{3,(m+1)\Delta t}^2/\Delta t \quad (q_{3,(m+1)\Delta t} = y)$$

$$A_{3,k,y} = 0 \quad (q_{3,(m+1)\Delta t} < y).$$

Since pearlite nodules nucleate at an austenite grain boundary and can grow into either of the adjacent austenite grains, ΔV_3^e is given by equation (15).

RESULTS AND DISCUSSION

There have been many studies about the occurrence of Widmanstätten ferrite in steels as a function of the chemical composition, austenite grain size and cooling rate during continuous cooling transformation [e.g. 7, 21–23]. It is consequently well established that Widmanstätten ferrite is favoured in austenite with a large grain structure. This is probably because Widmanstätten ferrite is rarely found in isolation but often forms as secondary plates growing from allotriomorphic ferrite layers. The prior formation of allotriomorphic ferrite, which is favoured by a *small* grain size, enriches the untransformed residual austenite with carbon and reduces the volume fraction of residual austenite which can subsequently transform into Widmanstätten ferrite, so it is not surprising that a small

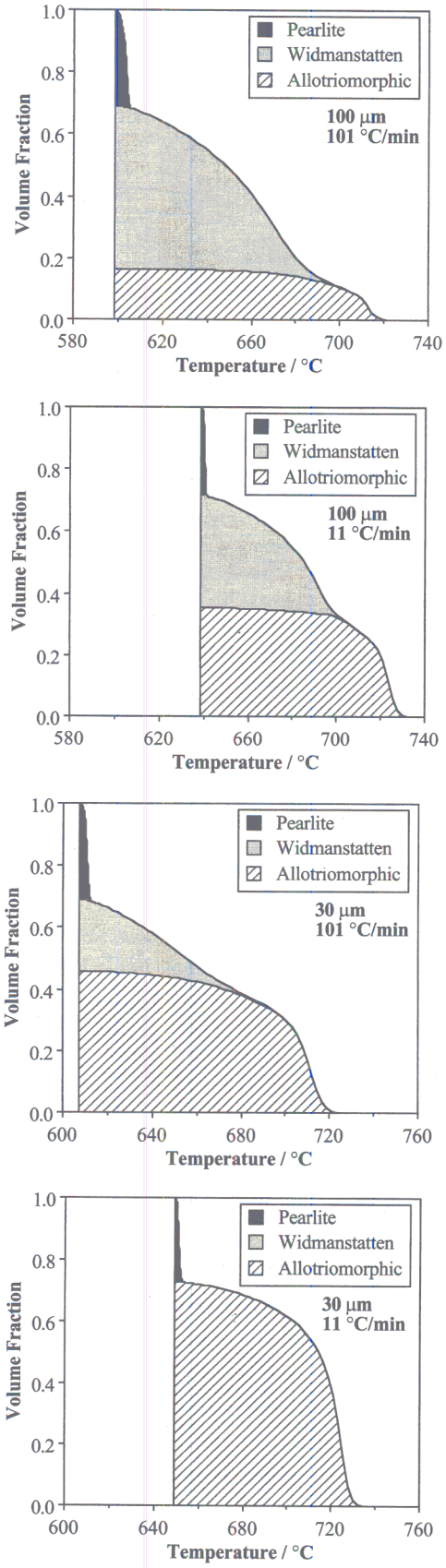

Fig. 5. Calculated evolution of microstructure as a function of the austenite grain size and cooling rate.

austenite grain size suppresses Widmanstätten ferrite. For the same reasons, an increase in the cooling rate will tend to favour the formation of Widmanstätten ferrite.

These and other concepts are implicitly built into the model presented here. This is because allotriomorphic ferrite, Widmanstätten ferrite and pearlite are allowed to grow together assuming that thermodynamic and kinetic conditions are satisfied. Their interactions are all taken into account during the course of transformation. It follows that it should be possible to reproduce the excellent quantitative data recently published by Bodnar and Hansen [7]. The present analysis is restricted to Fe–Si–Mn–C steel rather than the microalloyed steels also studied by Bodnar and Hansen.

The chemical composition of the steel is given in Table 1. They used heat-treatments which led to three different austenite grain sizes of 30, 55 and 100 μm. In addition, samples were cooled at five different rates; 11, 16, 30, 59 and 100°C/min.

Widmanstätten ferrite can nucleate directly from the austenite grain surfaces or indirectly from allotriomorphic ferrite–austenite interfaces. The present model includes both of these scenarios because of an approximation made in the formulation of extended area in equation (10). It is strictly not possible to separate out the contributions ΔO_j^e from each phase (for all values of y) when the phases grow at different rates. The result of the approximation is therefore to allow Widmanstätten ferrite to form even if the entire austenite grain surface is decorated with allotriomorphic ferrite. This is approximately equivalent to the secondary nucleation of Widmanstätten ferrite and pearlite on allotriomorphic ferrite.

The reasonable overall level of agreement between experiment and theory is illustrated in Fig. 4, for all of the data from Ref. [7]; the quantitative data plotted in Fig. 4 are also included in Table 2 since the complete details cannot be included in the plot. In all cases where the allotriomorphic ferrite content is underestimated, the Widmanstätten ferrite content is overestimated. This is expected both because the composition of the austenite changes when allotriomorphic ferrite forms and because its formation changes the amount of austenite that is free to transform to Widmanstätten ferrite.

MICROSTRUCTURE MAPS

Figure 5 show calculations which illustrate how the model can be used to study the evolution of microstructure as the sample cools. The calculations are for the steel composition stated in Table 2.

All of the generally recognised trends are reproduced. The amount of Widmanstätten ferrite clearly increases with the austenite grain size, and with the cooling rate within the range considered. Bodnar and Hansen [7] suggested that the effect of cooling rate on the amount of Widmanstätten ferrite

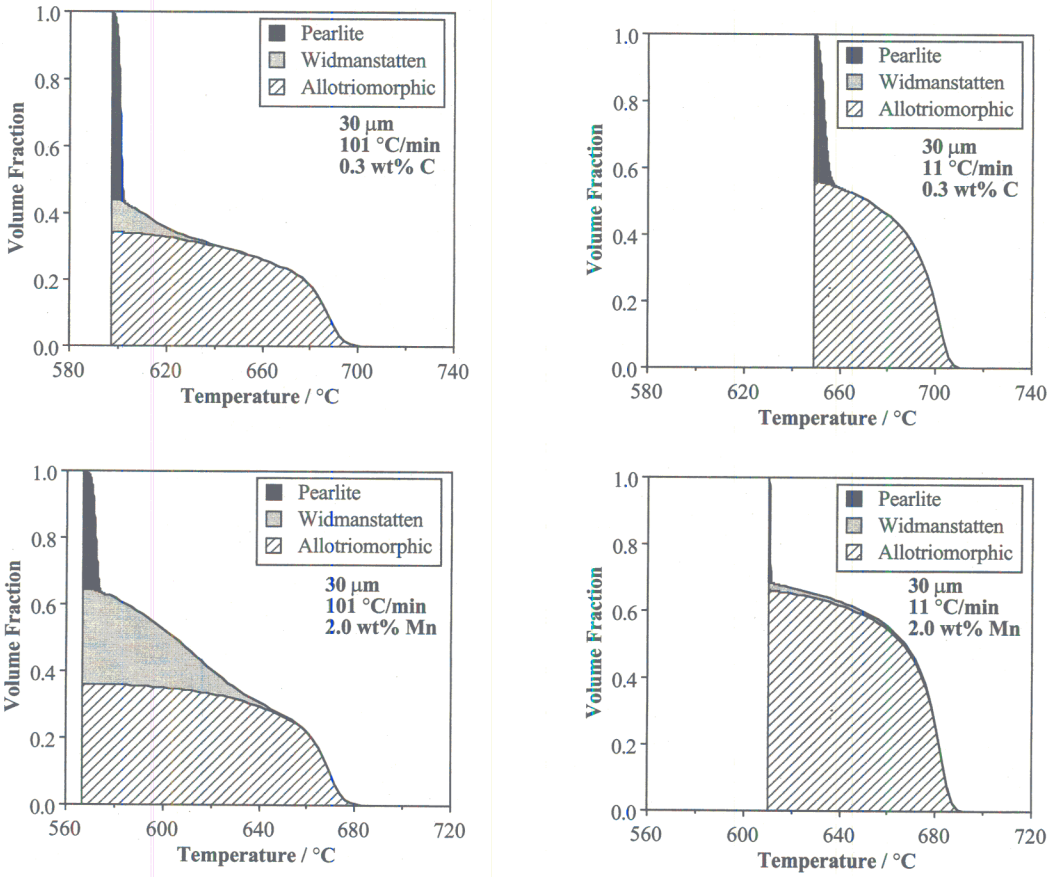

Fig. 6. Calculated evolution of microstructure as a function of the austenite grain size and the cooling rate. The steel composition is as given in Table 2, but with the carbon or manganese concentrations increased as indicated.

was smaller than that of the austenite grain size (for the values considered). This is also evident in Fig. 5.

The model also correctly predicts the influence of alloying elements such as carbon or manganese. At large cooling rates, Fig. 6 shows that an increase in the carbon concentration reduces the amount of Widmanstätten ferrite; this is because of the reduction in the temperature at which the Widmanstätten ferrite first nucleates and also by suppressing its growth rate.† The suppression of transformation temperatures also reduces the concentration of carbon in the residual austenite at which the formation of pearlite begins, since the $\gamma/\gamma + \theta$ has a positive slope on a plot of temperature vs carbon concentration. The fraction of pearlite is therefore increased in the microstructure.

The effect of carbon at the slower cooling rate is mainly to suppress the formation of allotriomorphic ferrite and hence to increase the proportion of pearlite (Fig. 6). At the austenite grain size of 30 μm and a cooling rate of 11°C/min, Widmanstätten ferrite is essentially absent at both the carbon concentrations studied.

An increase in the concentration of manganese to 2 wt% (Fig. 6) has a different effect because the effect on the pearlite transformation is less pronounced than carbon. Thus, the suppression of allotriomorphic ferrite permits a greater degree of transformation to occur to Widmanstätten ferrite.

SUMMARY

The classical Johnson–Mehl–Avrami theory for overall transformation kinetics has been successfully adapted to deal with the simultaneous formation of allotriomorphic ferrite, Widmanstätten ferrite and pearlite. A comparison with published experimental data has shown that the model developed is reasonable both quantitatively and with respect to well-established trends. The model can now be used to study theoretically the evolution of microstructure as a function of the alloy composition, the austenite grain size and the cooling conditions. Further work is needed to include other phases such as bainite, and to deal with microalloying additions. It would also be

†For an austenite grain size of 30 μm, a cooling rate of 101 K/min, Widmanstätten ferrite formation is suppressed to 693°C (from 725°C) with the increase in carbon concentration. Similarly, the growth rate of Widmanstätten ferrite at 675°C is reduced approximately by a factor of four with the increase in carbon concentration.

interesting to incorporate nucleation sites other than austenite grain surfaces.

Acknowledgements—We are grateful to the Engineering and Physical Sciences Research Council, and British Steel plc. for supporting this work. It is a pleasure to acknowledge some very helpful discussions with Dr Graham Thewlis. HKDHB is grateful to the Royal Society for a Leverhulme Trust Senior Research Fellowship.

REFERENCES

1. Christian, J. W., *Theory of Transformations in Metals and Alloys*, Part I, 2nd edn. Pergamon Press, Oxford, 1975.
2. Bhadeshia, H. K. D. H., In *Mathematical Modelling of Weld Phenomena III*, ed. H. Cerjak and H. K. D. H. Bhadeshia. Institute of Materials, London, 1996, pp. 1–50.
3. Watson, J. D. and McDougall, P. G., *Acta metallurgica*, 1973, **21,** 961.
4. Bhadeshia, H. K. D. H., *Materials Science and Technology*, 1985, **1,** 497.
5. Bhadeshia, H. K. D. H., *Acta metallurgica*, 1981, **29,** 1117.
6. Rees, G. I. and Bhadeshia, H. K. D. H., *Materials Science and Technology*, 1992, **8,** 985.
7. Bodnar, R. L. and Hansen, S. S., *Metallurgical and Materials Transactions A*, 1994, **25A,** 763.
8. Umemoto, M., Hiramatsu, A., Moriya, A., Watanabe, T., Nanba, S., Nakajima, N., Anan, G. and Higo, Y., *ISIJ International*, 1992, **32,** 306.
9. Bhadeshia, H. K. D. H., Svensson, L.-E. and Gretoft, B., *Acta metallurgica*, 1985, **33,** 1271.
10. Cahn, J. W., *Acta metallurgica*, 1956, **4,** 449.
11. Jones, S. and Bhadeshia, H. K. D. H., unpublished research, University of Cambridge, 1996.
12. Hillert, M., in *Lectures in The Theory of Phase Transformations*, ed. H. I. Aaronson. TMS-AIME, Warrendale, PA, 1975, pp. 1–50.
13. Bhadeshia, H. K. D. H., Svensson, L.-E. and Gretoft, B., in *Welding Metallurgy of Structural Steels*, ed. J. Y. Koo. TMS-AIME, Warrendale, PA, 1987, pp. 517–530.
14. Bradley, J. R. and Aaronson, H. I., *Metallurgical Transactions A*, 1977, **8A,** 317.
15. Trivedi, R. and Pound, G. R., *Journal of Applied Physics*, 1967, **38,** 3569.
16. Olson, G. B. and Cohen, M., *Metallurgical Transactions A*, 1970, **7A,** 1897.
17. Rees, G. I. and Bhadeshia, H. K. D. H., *Materials Science and Technology*, 1992, **8,** 985.
18. Trivedi, R., *Metallurgical Transactions*, 1970, **1,** 921.
19. Hillert, M., *Jernkontorets Ann.*, 1957, **141,** 757.
20. Takahashi, M., Reaustenitisation from bainite in steels. Ph.D. thesis, University of Cambridge, 1992.
21. Mehl, R. F., Barrett, C. S. and Smith, D. W., *Translations of AIMME, Iron and Steel Division*, 1933, **105,** 215.
22. Aaronson, H. I., Eylon, D., Cooke, C. M., Enomoto, M. and Froes, F. H., *Scripta metallurgica*, 1989, **23,** 435.
23. Krahe, P. R., Kinsman, K. R. and Aaronson, H. I., *Acta metallurgica*, 1972, **20,** 1109.